Journal of Magnetism and Magnetic Materials 497 (2020) 166078

Contents lists available at ScienceDirect

Journal of Magnetism and Magnetic Materials

journal homepage: www.elsevier.com/locate/jmmm

Research articles

Influence of weak frustration on quench dynamics of 1D spin-1/2 ANNNI model

Hadi Cheraghi[a], Majid Jafar Tafreshi[a,*], Saeed Mahdavifar[b]

[a] Department of Physics, Semnan University, 35195-363 Semnan, Iran
[b] Department of Physics, University of Guilan, 41335-1914 Rasht, Iran

A B S T R A C T

In this work we study the dynamical quantum phase transition in the 1D spin-1/2 transverse axial next-nearest-neighbor Ising (ANNNI) model by employing the mean field Jordan-Wigner approach. The NNN interaction breaks the integrability of the ANNNI model. We have focused on the induced dynamical effects of the frustration on quench dynamics of the system. The approach helps us to diagonalize the Hamiltonian in the region where the frustration is weak and the analytical method is reliable. First, the non-analyticity of the rate function is analyzed. It is found that only by quenching across the quantum critical point, regular non-analyticitic behaviors at periodic instants are seen in the dynamics of the rate function. Here, our results confirm the existence of paramagnetic commensurate and paramagnetic incommensurate phases in the system. Second, the order parameter dynamics as a system's macroscopical property is investigated and the oscillatory behavior is reported. Third, the nonequilibrium dynamics of the quantum correlations as the entanglement and the quantum discord are studied. We have compared the efficiency of the quantum discord with respect to the entanglement in the detection of the occurrence of the dynamical quantum phase transition.

1. Introduction

In a real experiment on the dynamics of a quantum system, small perturbations play very important roles. In theory, it is manifested in the time reversal process where the concept of time is reversed using a negative time. The stability of time reversal can be understood by focusing on the fidelity between the state time-evolved ($|\Psi_1(t)\rangle$) by Hamiltonian without perturbation and the state time-evolved ($|\Psi_2(t)\rangle$) when the perturbation is added. Mentioned fidelity is known as the Loschmidt echo and defined as $|\langle\Psi_1(t)|\Psi_2(t)\rangle|^2$ [1].

Recently, based on one hand the Loschmidt echo and other hand the equilibrium statistical mechanics, a theory called dynamical quantum phase transition (DQPT) is introduced [2–4]. In fact, during the subsequent real-time evolution of the system following a sudden quench of a control parameter across the quantum critical point, the dynamical counterpart of the free-energy density exhibits non-analyticities at some instants of critical times. Formalism is as follows. First the system is prepared in the ground state $|\Psi_0\rangle$ of an initial Hamiltonian H_i. Then, at least one of the parameters of the Hamiltonian is changed suddenly at the initial time $t = 0$ and the Hamiltonian is changed into the H_f where the $|\Psi_0\rangle$ is not one of the it's eigenstates and the time evolution of the system is dictated by H_f.

One dimensional (1D) spin-1/2 integrable systems are very good candidates for study the DQPT. First of all, the DQPT is studied in the Ising model in a transverse field (ITF) [2,5–10]. In addition to the 1D ITF model, the DQPT was also studied in 1D spin-1/2 XXZ [11–16], XY [17,18], and Bose-Hubbard chain models [19]. From an experimental point of view, the first direct observation of a DQPT was reported in 2017 [20]. It was informed that the DQPTs are robust against modifications of microscopic details of the underlying Hamiltonian. With up to 53 trapped ion qubits, a direct probing of the DQPT was shown in the ITF model [21]. Appearance, movement and annihilation of dynamical vortices in momentum space after sudden quenches close to the quantum topological phase transition were also observed [22]. It was shown that dynamical vortices can be interpreted as dynamical Fisher zeroes of the Loschmidt amplitude, which signal a DQPT in a quantum system.

The 1D ITF model in the presence of the next-nearest neighbor (NNN) interaction is known as the spin-1/2 transverse axial NNN Ising model (ANNNI). The Hamiltonian of the ITF model in the presence of the NNN interaction can not be exactly diagonalized and thus the ground state phase diagram is not completely clear and is under investigation [23–35]. In the absence of the TF, based on the NNN interaction strength, the ground state of the system can be found in the ferromagnetic phase or in the anti-phase. In the presence of a TF, beside the ferromagnetic and anti-phase, different phases such as the paramagnetic and the floating phases have already been reported.

Since the integrability is lost in the ANNNI model, more intensive dynamical studies were invoked [36–39]. Using the numerical matrix product state methods the DQPT was investigated for quenches from

* Corresponding author.
E-mail address: mtafreshi@semnan.ac.ir (M. Jafar Tafreshi).

https://doi.org/10.1016/j.jmmm.2019.166078
Received 16 June 2019; Received in revised form 26 September 2019; Accepted 28 October 2019
Available online 31 October 2019
0304-8853/

the paramagnetic to the ferromagnetic phase [36]. It was found that, existence of non-analyticity in the rate function of the return probability (RFRP) is stable against the NNN interaction. Critical times where the RFRP becomes non-analytic do not show any periodicity. In addition some kinks have been observed in the RFRP behavior in quench dynamics of the system. By considering the NNN interaction as a perturbation term and using the continuous unitary transformations, the DQPT was studied from an analytical point of view [37]. Excellent agreement between the predictions of perturbations and the numerical matrix product state results was reported. In addition, it was analysed that how the location and shape of these non-analyticities are affected by the perturbing NNN interaction. Using the numerical density matrix renormalization group (DMRG), the dynamics arising from a double quench were also studied [38]. It was demonstrated that there is no relationship between the critical times after the second quench and the zeros of the magnetization. out-of-time-ordered (OTO) correlators of the order parameter in ANNNI model were also calculated numerically for a sudden quench [39]. It was argued that OTO correlators can be used to dynamically detect dynamical quantum critical points.

In this work we focus on the ANNNI model. Using the Jordan-Wigner mean-field (JW-MF) approach, the Hamiltonian is diagonalized in the thermodynamic limit. We have shown that the used analytical method is reliable in the region where the frustration is not strong. The ferromagnetic and paramagnetic phases are exist in the ground state phase diagram of the model which are separated by a quantum critical line. The transverse magnetic field is selected as the control parameter in quench dynamics. By selecting different values of the transverse magnetic field, the system is quenched between its quantum phases. We also consider quenches in the same quantum phases. In all cases, the non-equilibrium dynamics of the rate function, Fischer zeros, macroscopic order parameters and microscopic quantum correlations as the pairwise entanglement and the quantum discord are analyzed.

The rest of the paper goes in the following sequence. In Section 2 the Hamiltonian is introduced and using the JW-MF approach, it is diagonalized to obtain its spectrum. In Section 3, results on the RFRP and Fisher zeroes are presented for quenches crossed of the critical points. In addition, it is shown that how frustration affects the wave number of quasiparticle excitations and the critical times. In this section as an added part, we also consider the dynamics of the spin-spin correlation function and the magnetization. Finally, in Section 4 the dynamics of entanglement and quantum discord are studied.

2. ANNNI model

The Hamiltonian of the 1D spin-1/2 transverse axial next-nearest neighbor Ising (ANNNI) model is defined as

$$\mathscr{H} = -J\sum_{n=1}^{N}\ [S_n^x S_{n+1}^x - \Delta S_n^x S_{n+2}^x + hS_n^z], \tag{1}$$

where S_n is the spin-1/2 operator on the n-th site, $J > 0$ denotes the ferromagnetic (FM) nearest-neighbor interaction, Δ is the an antiferromagnetic (AFM) second-neighbor interaction and h is the TF strength. The $\Delta > 0$ is called the frustration parameter. It is known that for $\Delta = 0$, the model transfers to the ITF, which can be mapped to a system of free fermions and therefore be solved exactly [40]. In this case, there is a FM to paramagnetic (PM) second order quantum phase transition at $h_c = \frac{J}{2}$ so that for value of magnetic field closed to the quantum critical point, the correlation length ξ diverges as $\xi \sim |h - h_c|^{-\upsilon}$ with $\upsilon = 1$. On the other hand, for $h = 0$ (classical ANNNI chain), the ground state is FM for $\Delta < 0.5$ and anti-phase (AP) $(|{+}{+}{-}{-}...\rangle)$ for $\Delta > 0.5$, with a multicritical point, the Lifshitz point, at $\Delta = 0.5$ so that at this point, the ground state has very high degeneracy where for large values of N (which is the size of the system) it is as $\sim g^N$ with golden ratio $g = \frac{\sqrt{5}+1}{2}$. The quantum phase transition between the PM and the FM belongs to the Ising universality class and for values of frustration less than 0.5 is located at [30,24]

$$\frac{1}{2} - \Delta = h_c - \frac{\Delta h_c^2}{1-\Delta}, \tag{2}$$

which is also called the Peschel-Emery one-dimensional line. Using the analytical fermionization approach, the ANNNI model can be mapped to a system of interacting fermions which cannot be solved exactly. The phase diagram of this model has been studied by several methods. Although as one can find out, there is not a consensus on the ground-state phase diagram of this model but almost all works agree with existence of a floating phase (FP) in the system which is located between the anti-phase and the PM ($\Delta > 0.5$). In addition, there are suggestions that the PM phase is divided into two parts, paramagnetic commensurate (PC) with monotonically decaying and paramagnetic incommensurate (PI) with oscillatory decaying [26,30].

As we have mentioned the Hamiltonian can be diagonalized approximately. By applying the Jordan-Wigner transformation

$$\begin{aligned} S_n^+ &= a_n^\dagger\left(e^{\,i\pi\sum\limits_{l<n} a_l^\dagger a_l}\right),\\ S_n^- &= \left(e^{\,-i\pi\sum\limits_{l<n} a_l^\dagger a_l}\right)a_n,\\ S_n^z &= a_n^\dagger a_n - \tfrac{1}{2}, \end{aligned} \tag{3}$$

the Hamiltonain converts from spin operators into the spinless fermionic operators as

$$\begin{aligned} \mathscr{H} &= -\frac{J}{4}\sum_{n=1}^{N}(a_n^\dagger a_{n+1}^\dagger + a_n^\dagger a_{n+1} + h.\,c.) + \frac{J\Delta}{4}\\ &\sum_{n=1}^{N}(a_n^\dagger a_{n+2}^\dagger + a_n^\dagger a_{n+2} + h.\,c.) - \frac{J\Delta}{2}\sum_{n=1}^{N}(a_n^\dagger a_{n+2}^\dagger + a_n^\dagger a_{n+2} + h.\,c.)\\ &(a_{n+1}^\dagger a_{n+1}) - Jh\sum_{n=1}^{N}\left(a_n^\dagger a_n - \frac{1}{2}\right). \end{aligned} \tag{4}$$

Now, using Wick's theorem [41] for decomposing the fermion interaction terms to some order parameters which are related to the two-point correlation functions as

$$\gamma_p = \langle a_n^\dagger a_{n+p-1}\rangle\ ;\ \gamma_q = \langle a_n^\dagger a_{n+q-3}^\dagger\rangle, \tag{5}$$

where $p = 1, 2, 3$ and $q = 4, 5$. Performing a Fourier transformation as $a_n = \frac{1}{\sqrt{N}}\sum_k e^{-ikn}a_k$, and also Bogoliubov transformation as

$$a_k = \cos(\theta_k)\beta_k + i\sin(\theta_k)\beta_{-k}^\dagger, \tag{6}$$

the Hamiltonian will be diagonalized as

$$\mathscr{H} = \sum_{k>0}\varepsilon_k\Big(\Delta, h\Big)(\beta_k^\dagger\beta_k - \beta_{-k}\beta_{-k}^\dagger), \tag{7}$$

where the energy spectrum is

$$\begin{aligned} \varepsilon_k(\Delta, h) &= \sqrt{\mathscr{A}_k^2(\Delta, h) + \mathscr{B}_k^2(\Delta, h)},\\ \mathscr{A}_k(\Delta, h) &= -J\Big[\tfrac{1}{2}\cos(k) + h - \tfrac{\Delta}{2}\cos(2k)(1-2\gamma_1) - 2\Delta\cos(k)(\gamma_2+\gamma_4)\\ &\quad + \Delta(\gamma_3+\gamma_5)\Big],\\ \mathscr{B}_k(\Delta, h) &= -J\Big[\tfrac{1}{2}\sin(k) - \tfrac{\Delta}{2}\sin(2k)(1-2\gamma_1) - 2\Delta\sin(k)(\gamma_2+\gamma_4)\Big], \end{aligned} \tag{8}$$

and $\tan\Big(2\theta_k\Big(\Delta, h\Big)\Big) = -\frac{\mathscr{B}_k(\Delta,h)}{\mathscr{A}_k(\Delta,h)}$. It should be noted that the mean field order parameters derived from following equations corresponding to the ground state of ANNNI model should be satisfied self-consistently

$$\gamma_p = \frac{1}{2}\delta_{1,p} - \frac{1}{2N}\sum_k \cos((p-1)k)\frac{\mathscr{A}_k(\Delta,h)}{\varepsilon_k(\Delta,h)},$$
$$\gamma_q = \frac{1}{2N}\sum_k \sin((q-3)k)\frac{\mathscr{B}_k(\Delta,h)}{\varepsilon_k(\Delta,h)}. \quad (9)$$

Since the mentioned self-consistent equation falls in the region $\Delta \geqslant 0.5$, our following study is restricted to the region $\Delta < 0.5$ [28].

3. Dynamical quantum phase transition

The phase transitions in a thermodynamic system are marked by the non-analyticities in the free-energy density, which can be obtained by analyzing the zeros of the partition function where they are appeared by a crossing the imaginary axis in a complex temperature plane proposed by Fisher [42] or in a complex magnetic plane proposed by Lee-Yang [43]. From similarity, Heyl *etal*. [2] introduced a connection between the Loschmidt echo and the non-analyticities in the dynamics of free energy in the complex time plane known as DQPTs. They considered a one-dimensional ITF model and suggested that DQPTs situate only if a performed quench crosses from an equilibrium quantum critical point. However, Further studies revealed that DQPTs can occur for quenches within the same phase [17,44] or cannot occur for quenches crossed from an equilibrium quantum critical point [45].

To investigate a physical system out of equilibrium, the simplest controllable scheme is based on using the sudden change of control parameters. To do that, we put the system in an equilibrium state described with the Hamiltonian $\mathscr{H}_i = \sum_k \mathscr{H}_k^i$ and the initial state $|\Psi_0\rangle$. Afterwards, we suddenly change the control parameters from their initial values to their final values. Final Hamiltonian and its time-evolved state will be described as $\mathscr{H}_f = \sum_k \mathscr{H}_k^f$ and $|\Psi(t)\rangle = e^{-i\mathscr{H}_f t}|\Psi_0\rangle$, respectively. In this case, the Loschmidt echo defines as $LE(t) = \prod_k \mathscr{L}_k(t)$ where

$$\mathscr{L}_k(t) = \langle\Psi_0| e^{-iH_f^k t}|\Psi_0\rangle. \quad (10)$$

Need to be mentioned, the Loschmidt echo is not uniquely defined when the ground-state manifold of the initial Hamiltonian is degenerate [46]. Let $\{\beta_k^\dagger, \beta_k\}$ and $\{\eta_k^\dagger, \eta_k\}$ denote the fermionic species diagonalising $H(\Delta_i, h_i)$ and $H(\Delta_f, h_f)$ with the vacuum ground state $|0\rangle_{\beta_k}$ and $|0\rangle_{\eta_k}$ respectively. Then, for ANNNI model we have

$$\mathscr{H}(\Delta_i, h_i) = \sum_k \varepsilon_k^i\left(\beta_k^\dagger\beta_k - \frac{1}{2}\right),$$
$$\mathscr{H}(\Delta_f, h_f) = \sum_k \varepsilon_k^f\left(\eta_k^\dagger\eta_k - \frac{1}{2}\right), \quad (11)$$

where $|0\rangle_{\beta_k}$ is related to the $|0\rangle_{\eta_k}$ through [47,48]

$$|0\rangle_{\beta_k} = \lambda^{-1} e^{-i\sum_{k>0}\tan(\Phi_k)\eta_k^\dagger\eta_{-k}^\dagger}|0\rangle_{\eta_k}, \quad (12)$$

and $\Phi_k = \theta_k^f - \theta_k^i$ is the difference between the Bogoliubov angles diagonalizing the pre-quench and post-quench Hamiltonians, respectively. It should be noted that for quench from $\Delta_i, h_i \to \Delta_f, h_f$, the self-consistent relations should be solved numerically for both initial and final points. It is straightforward to show that the Loschmidt echo corresponding to the ground state of the ANNNI model is given by

$$LE(t) = \prod_{k>0}(\cos^2(\Phi_k) + \sin^2(\Phi_k)e^{-2it\varepsilon_k^f}). \quad (13)$$

It is known that the Loschmidt echo typically decreases with passing time [49,50]. In fact, it has been shown there are three consecutive stages of the time-decay of the Loschmidt echo. Anyway, the DQPT was discovered with the formal similarity of the partition function $Z(\beta) = tr(e^{-\beta H})$ which is bounded by the initial state $|\Psi_0\rangle$ as $Z(z) = \langle\Psi_0| e^{-zH}|\Psi_0\rangle$ with $z \in \mathbb{C}$ so that it represents the Loschmidt amplitude as $LA(t) = \langle\Psi_0|e^{-iHt}|\Psi_0\rangle$ for $z = it$ that is the modulus of the Loschmidt echo. Likewise, the DQPTs are defined as the rate function of the return probability (RFRP) as

$$r(t) = -\lim_{N\to\infty}\frac{1}{N}\log\left|LE(t)\right|^2. \quad (14)$$

One can show easily that

$$r(t) = -\frac{2}{N}\sum_{k>0}\log|\cos^2(\Phi_k) + \sin^2(\Phi_k)e^{-2it\varepsilon_k^f}|. \quad (15)$$

DQPTs take place in the critical times where the Fisher zeroes exist [42]. The Fisher zeroes, $z_n(k)$, in the complex plane coalesce to a family of lines labeled by a number $n \in \mathbb{Z}$

$$z_n(k) = \frac{1}{2\varepsilon_k^f}[\ln(\tan^2(\Phi_k)) + i\pi(2n+1)]. \quad (16)$$

Hence, the critical points appear periodically at the critical times

$$t_n^* = \frac{\pi}{\varepsilon_{k^*}^f}\left(n + \frac{1}{2}\right), \quad n = 0, \pm1, \pm2, \ldots \quad (17)$$

where the dispersion relation is given by $\varepsilon_{k^*}^f$ with k^* which is a particular mode that leads to vanishing the logarithm in (15) at $t = t_n^*$ and is determined by

$$\mathscr{A}_{k^*}(\Delta_i, h_i)\mathscr{A}_{k^*}(\Delta_f, h_f) + \mathscr{B}_{k^*}(\Delta_i, h_i)\mathscr{B}_{k^*}(\Delta_f, h_f) = 0. \quad (18)$$

The dynamics of a many body quantum system typically involve many excited eigenstates with a non-thermal distribution. Among the excited eigenstates whose their wave numbers include k^*, play a role in DQPTs of the system. For finding k^* and examining the impact of frustration Δ on it, let us rewrite (15) as

$$r(t) = -\frac{1}{N}\sum_{k>0}\log[1 - \lambda_k\sin^2(\varepsilon_k^f t)], \quad (19)$$

where $\lambda_k = \sin^2(2\Phi_k)$. In particular, at critical times it should be $\sin^2(\varepsilon_{k^*}^f t_n^*) = 1$, thus, nonanalyticities in the RFRP appear at $\lambda_{k^*} = 1$.

At first, for checking the validity of the JW-MF approach in DQPT of the ANNNI model, we have calculated the rate function for some special quenches in accordance with what is reported in Ref. [36]. Results are presented in Fig. 1. In fact, a quench from the paramagnetc to the ferromagnetic phase for different values of the frustration $\Delta = 0.05, 0.15$ is considered. As is clearly seen, there is a very good agreement between our analytical JW-MF results and the numerical DMRG results.

In Fig. 2(a) we have plotted λ_k versus k/π for quench from $h_i = 0.1$ to $h_f = 2.0$ for different values of the frustration Δ. It obviously shows for a greater value of frustration, DQPT happens in a greater value of the wave number k^*. More, the increment of the frustration reduces the value of wave number for $k < k^*$ and enhances it for $k > k^*$. In addition, we have found for weak frustration, the wave number k^* has approximately a linear relation with respect to the frustration Δ (see the inset in Fig. 2(a)). These results for λ_k and k^* are exactly the same as quench from $h_i = 2.0$ to $h_f = 0.1$. This symmetry is explicit from (18) where it remains unchanged under the transformation $i \leftrightarrow f$.

As a result, with the use of (8), (17) and (18) and defining $t^*\left(\Delta_i, h_i, \Delta_f, h_f\right) = \frac{\pi}{\varepsilon_{k^*}^f}$, it seems to be no simple quantitative relation but possible to write

$$t_n^* = t^*\left(\Delta_i, h_i, \Delta_f, h_f\right)\left(n + \frac{1}{2}\right), \quad (20)$$

that shows the critical times depend on the initial and final values of Δ and h. For searching the impact of the frustration at the critical times, in Figs. 2(b & c), we have indicated the first critical time t^* versus Δ. While Fig. 2(b) reveals the existence a linear relation for t^* versus Δ for quench from $h_i = 0.1$ to $h_f = 2.0$, Fig. 2(c) discloses approximately a linear relation comes out for quenching from $h_i = 2.0$ to $h_f = 0.1$ for large enough values of the frustration.

As discussed in the Introduction, in a numerical study with DMRG, C. Karrasch and D. Schuricht investigated DQPTs as calculating the

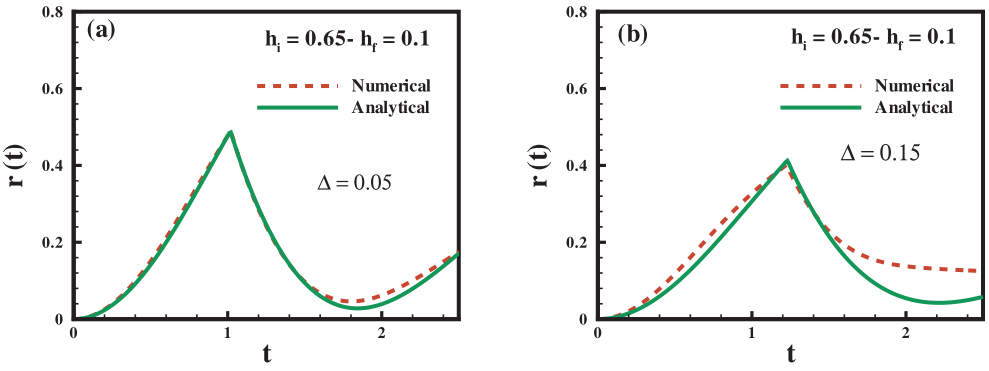

Fig. 1. The time evolution of the rate function for quench from FM to PM phase for different values of weak frustration (a) $\Delta = 0.05$ (b) $\Delta = 0.15$. As is seen analytical JW-MF results are in a very good agreement with the numerical DMRG results presented in Ref. [36].

RFRP for the ANNNI model for both weak and strong frustrations [36]. They focused on the issue to show the non-analyticities in the time evolution of the RFRP are stable against integrability-breaking interactions. An imprint of these results was done in view of the presence of Δ as perturbation for $\Delta < 0$ (the non-frustrated model) in the DQPTs of ANNNI model [37]. In the following part of this paper, we again revisit this idea, but for weak frustration, $0 \leqslant \Delta < 0.5$, using Jordan-Wigner mean-field approach results. We will show that the presence of the weak frustration can have a dramatic effect in the case of the non-equilibrium dynamics of the system.

In order to consider the influence of the presence of the frustration in DQPTs of ANNNI model, the RFRP and Fisher zeroes for $n = 1$ have been plotted in Fig. 3 for different values of frustration, $\Delta < 0.5$, in quenching from $h_i = 0.1$ to $h_f = 2.0$ (FM to PM) and vice versa. All these quenches crosses from quantum critical points. We clearly observe non-analyticities. For quench from FM to PM for $h_i = 0.1$ to $h_f = 2.0$, Fig. 3(a), increase in the frustration values leads to increase in the critical times' values. Additionally, fluctuations of steady states start to enhancement. It has been shown that the correlation functions in the two parts of the PM phase have different behaviors. The correlation functions in PC phase decay monotonically with distance without any oscillation while in PI phase, they decay as oscillatory [26,30]. Indeed, this study indicates that since the quenched point is in PC phase ($\Delta = 0.0, 0.1, 0.2$), it leads the system goes to the equilibrium steady state. On the contrary, for stronger frustration such a way the quenched point is in PI phase ($\Delta = 0.3, 0.4$) because the fluctuations are enhanced, the steady states are not achieved even at $t \to \infty$. For Fisher zeroes as shown in Fig. 3(b), enhancing Δ enhances a bit values of them.

On the other hand, Fig. 3(c & d) indicate quenches originating from PM to FM for $h_i = 2.0$ to $h_f = 0.1$. For Fisher zeroes, outcomes for quench from PM to FM are the same as quench from FM to PM. On the other side, for the RFRP, increment the frustration values decrements the maximum and minimum values of the RFRP (that this behavior is vice versa from quench from FM to PM) and increments the critical times' values. Furthermore, increment the frustration values decrease the fluctuations of steady states which means that the time evolution is not longer and the RFRP becomes smooth and goes to its steady state faster. In this case, quench from PM to FM, all quenches put in an equilibrium steady state at $t \to \infty$. As a consequence, the existence of non-analyticities for both FM to PM and PM to FM quenches is stable against the value of the weak frustration, which is in a good agreement with Ref. [37]. Consequently, for both of these two quenches, the shape and locations of the cusps appear to depend on the value of the frustration in a regular way, even at long times and for a range of the frustration strengths.

In addition, to be more precise to make a connection between DQPT and zero-temperature quantum phase transition, we have calculated the equilibrium value of the RFRP (r_{eq}) for quenching from $h_i = 0.1$ and $h_i = 2.0$ to desired magnetic field in the range of $h_f \in [0.2, 2]$ and $h_f \in [0.1, 1.9]$, respectively. Results are presented in Figs. 3(e & f). It is completely clear from Fig. 3(e) that the equilibrium value of the RFRP for quench from FM to PM has a jump on $h_f = h_c$ and afterward by increasing value of h_f it asymptotically tends to a constant value. Explicitly, the greater the amount of frustration for $h_f < h_c$ ($h_f > h_c$) takes the greater (the lower) equilibrium value. Besides, when a quench starts from $h_i = 2.0$ to h_f, Fig. 3(f), by reducing h_f from 1.9 to 0.1, the equilibrium value of the RFRP increases and finds a maximum at $h_f = h_c$. After that, for $h_f < h_c$ for $\Delta = 0.0, 0.1, 0.2$, where final point is located

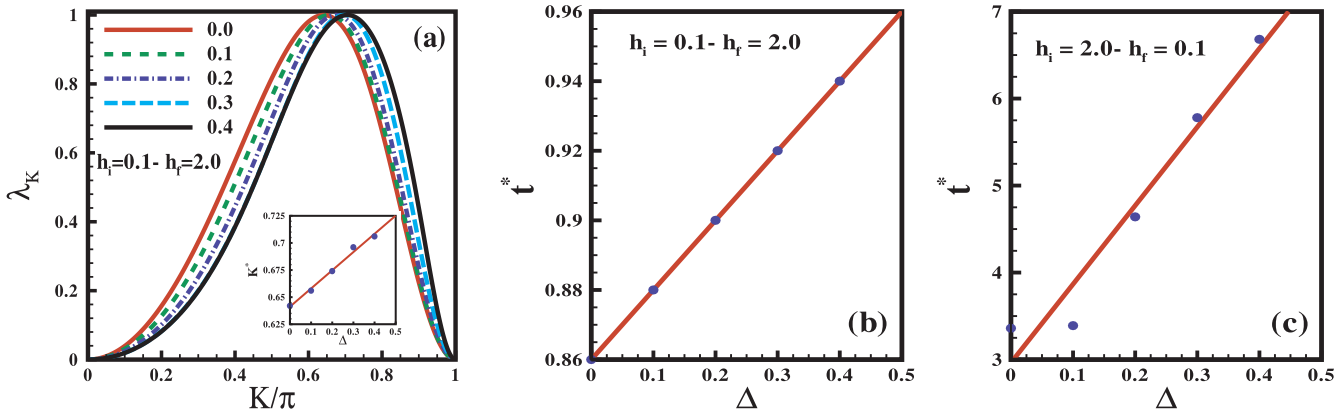

Fig. 2. (a) The value of λ_k versus k/π for quench from $h_i = 0.1$ to $h_f = 2.0$ for different values of frustration for Δ: $0.0 \to 0.4$ (from red to black). It explicitly shows the effect of frustration to the wave number k^*. Also, the inset figure reveals there is approximately a linear relation between k^* and Δ. (b) and (c) display the first critical time versus Δ for quench from $h_i = 0.1$ to $h_f = 2.0$ and its vice versa respectively. (For interpretation of the references to colour in this figure legend, the reader is referred to the web version of this article.)

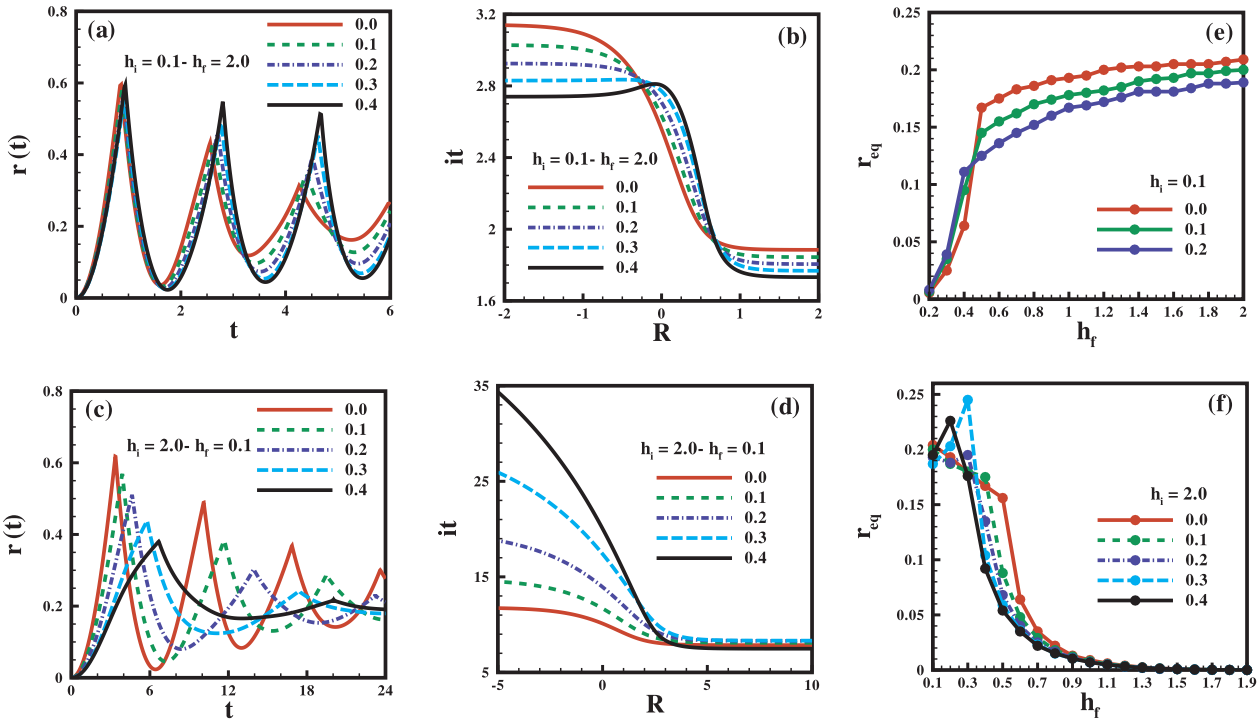

Fig. 3. The time evolution of the rate function for quench (a) from FM to PM and (c) PM to FM and their Fisher zeroes for $n = 1$, (b) and (d), for different values of weak frustration from 0.0 to 0.4 (from red to black), respectively. Fig. (a) clearly shows for quench from FM to PM, the bigger values of frustration create bigger fluctuations and does not allow for the system to go to an equilibrium state. In contrast, Fig. (c) reveals for quench from PM to FM, the bigger values of frustration destroy fluctuations and let the system going to equilibrium state faster. (e) and (f) show the values of the equilibrium rate function versus h_f for quenches from $h_i = 0.1$ and $h_i = 2.0$, respectively. In both Figs, we see signs of crossing quenches from critical fields as (e) jumping on and (f) for $\Delta = 0.0, 0.1, 0.2$ jumping on and for $\Delta = 0.3, 0.4$ maximizing at h_c. (For interpretation of the references to colour in this figure legend, the reader is referred to the web version of this article.)

in PM phase, equilibrium value enhances but for $\Delta = 0.3, 0.4$, where final point is located at PI phase, it reduces. We interpret these behaviors as an imprint of the existence of PC and PI phases in the ground state phase diagram of the system.

In a separate case, to find out another insight on the impact of the frustration in quench dynamics of ANNNI model, in the following, we focus on the dynamics of spin–spin correlation function, $S^{xx}_{n,n+1}(t) = < S^x_n(t)S^x_{n+1}(t)>$, and the magnetization $M_z(t)$, which can be observed easily through experiment. It should be noted that the magnetization along the X-axis is proportional to the mentioned spin–spin correlation function. We will show how the presence of frustration can increase or destroy oscillation of the dynamics of these observables. By using (25) and (26) the mentioned functions can be obtained as

$$\begin{aligned} M_z(t) &= P_{m=0}(t) - \frac{1}{2} \\ S^{xx}_{n,n+1}(t) &= \frac{1}{2}\{P_{m=1}(t) + \mathrm{Re}[T_{m=1}(t)]\} \end{aligned} \tag{21}$$

where $Re[...]$ denotes the real part. First, we investigate quench from $h_i = 2.0$ where the initial state is in the PM phase. In this phase, all the spins aligned along the X-axis and the magnetization in the x direction shows the ordering. Fig. 4 shows the results of quenches to a final $h_f = 0.1$ for different values of the frustration $\Delta < 0.5$. One should note that in the quenched point, the ground state has a different symmetry and spins are aligned along the Z-axis. The analytical data in Figs. 4(a & b) illustrate the oscillatory decay of magnetization along the Z and X axes for all frustration values occurs which is in complete agreement with what was found for spin-1/2 XXZ chain model [11]. In Fig. 4(c), we have plotted the spin–spin correlation function and the magnetization along the Z-axis for values of the frustration $\Delta = 0.3, 0.4$. Since the system is quenched into a region where the steady state expected to have FM ordering along the Z-axis, the initial behavior of time evolution for the magnetization is increasing but for the spin–spin correlation is decreasing. In addition, at the same times oscillations are seen.

4. Quantum correlations

One of the most interesting features of quantum mechanics is quantum correlations (QCs) which have been regarded as a key resource to detect and understand properties of complex many-body systems specially to reveal their critical points (CP) [51–56]. Compared with the great development of studying quantum phase transitions in equilibrium systems, the understanding of the non-equilibrium DQPTs is still inadequate. Some investigations have been carried out to study dynamical quantum correlations in integrable and non-integrable models [57–62] but to the best of our knowledge, ANNNI model has not been explored for the view of dynamical quantum correlations. Our particular interest is to draw the distinct signatures of quenched system manifested in the dynamics when a quench crosses from CP in the presence of the frustration. In this way, we write the reduced density matrix in terms of two-point fermionic correlation functions by solving a set of self-consistent equations and employ concurrence and quantum discord (QD) as measures of QCs [63–65]. The concurrence measures the nonlocal quantumness of correlations while QD measures the total amount of QCs of a state. In other words, QD shows the existence of QCs where concurrence shows that the system is separable. Accordingly, the QD can be different from zero even if a quantum system is separable.

The concurrence between two spins at site i and j can be obtained from the corresponding reduced density matrix ρ_{ij} [63,64]. In the fermionic picture with two-point correlation functions, one can write the reduced density matrix for the pairs in the distance m, $(i, j = i + m)$ as [66]

$$\rho_{i,i+m} = \begin{pmatrix} X^+_{i,i+m} & 0 & 0 & -f^*_{i,i+m} \\ 0 & Y^+_{i,i+m} & Z^*_{i,i+m} & 0 \\ 0 & Z_{i,i+m} & Y^-_{i,i+m} & 0 \\ f_{i,i+m} & 0 & 0 & X^-_{i,i+m} \end{pmatrix}. \tag{22}$$

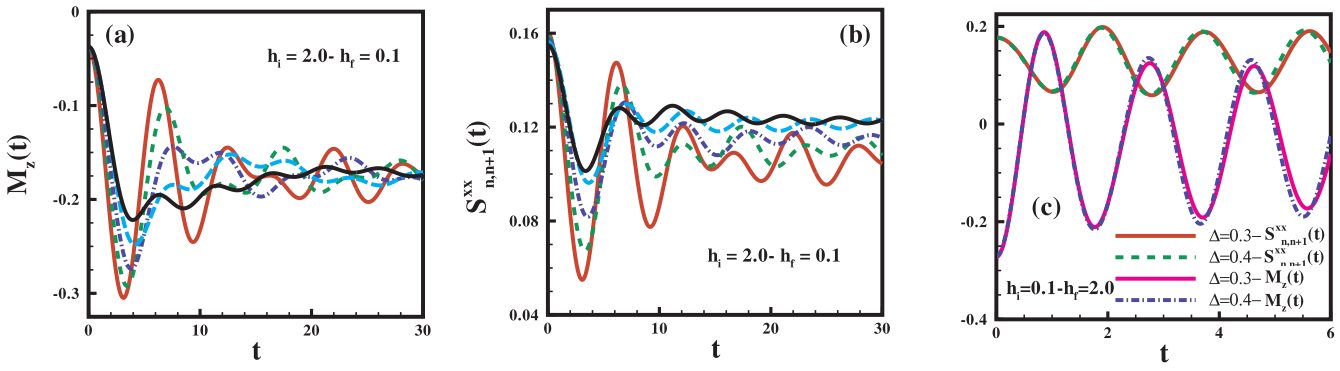

Fig. 4. Quench dynamics of two observables (a) magnetization $M_z(t)$, (b) order parameter $S^{xx}_{n,n+1}$, from $h_i = 2.0$ to $h_f = 0.1$ for different values of the frustration Δ: $0.0 \rightarrow 0.4$ (from red to black) and (c) both of them from $h_i = 0.1$ to $h_f = 2.0$ for $\Delta = 0.3, 0.4$. (For interpretation of the references to colour in this figure legend, the reader is referred to the web version of this article.)

Calculations of the reduced density matrix elements are explained in Appendix in details. The concurrence between two spins at sites i and $i + m$ will be obtained by

$$C(\rho_{i,i+m}) = \max\{0, \sqrt{\lambda_1} - \sqrt{\lambda_2} - \sqrt{\lambda_3} - \sqrt{\lambda_4}\} \tag{23}$$

where λ_i are the eigenvalues of $R = \rho\widetilde{\rho}$ matrix in decreasing order and $\widetilde{\rho}_{i,i+m} = (\sigma^y_i \otimes \sigma^y_{i+m})\rho^*_{i,i+m}(\sigma^y_i \otimes \sigma^y_{i+m})$. $\rho^*_{i,i+m}$ is the conjugate of $\rho_{i,i+m}$ and σ^y is the y component of the Pauli operator. On the other side, QD is defined by difference of total correlation, $\mathscr{I}(\rho_{i,i+m})$, and classical correlation, $\mathscr{C}(\rho_{i,i+m})$ as [67]

$$QD_{i,i+m} = \mathscr{I}(\rho_{i,i+m}) - \mathscr{C}(\rho_{i,i+m}). \tag{24}$$

The calculation of two sites reduced density matrix requires knowledge of time-dependent two-point correlation functions, which can be obtained for a given distance, m, from the following equations

$$\begin{aligned} P_m(t) &= \frac{1}{N}\sum_{l=1}^{N} < a_l^\dagger a_{l+m} > \\ &= \frac{1}{N}\sum_{k>0} \cos(km)[1 - \cos(2\theta_k^f)\cos(2\Phi_k)\sin(2\theta_k^f)\sin(2\Phi_k)\cos(2\varepsilon_k^f t)], \end{aligned} \tag{25}$$

and

$$\begin{aligned} T_m(t) &= \frac{1}{N}\sum_{l=1}^{N} < a_l^\dagger a_{l+m}^\dagger > \\ &= \frac{1}{N}\sum_{k>0} \sin(km)\sin\left(2\Phi_k\right)\left[\frac{\sin(2\theta_k^f)}{\tan(2\Phi_k)} - \cos\left(2\theta_k^f\right)\cos\left(2\varepsilon_k^f t\right)\right. \\ &\quad \left. - i\sin(2\varepsilon_k^f t)\right]. \end{aligned} \tag{26}$$

Throughout of this part our mean of QCs is QCs between the first neighbor spin pairs because for further distances, their values for ANNNI model in the region of weak frustration are zero. To understand more deeply about the temporal initial behavior of QCs and the amount of their steady states when the quench is done within the same phase, into and crossed from critical point, first of all, let us consider the ITF model in the absence of the frustration ($\Delta = 0$).

In Figs. 5(b & d) concurrence and QD and in Figs. 5(b & d) their density-plots as a function of time and final magnetic field h_f for quenching from $h_i = 0.1$, where the initial state of the system is in the FM phase, to different final values of $h_f = [0.3, 0.7]$ and desired h_f are plotted, respectively. For the quenching within the FM phase, the concurrence, first increases with time to its maximum value, subsequently reduces and by performing some oscillations tends to a constant value for large time. Instead, for the quenches into and crossed from CP, the concurrence, first decreases with time, reaches to a minimum value after a short time, then increases and finally starts to oscillate. Accordingly, this initial behavior of time evolution of concurrence i.e., to increase for $h_f < h_c$ and to decrease for $h_f > h_c$ when quench starts from FM phase, is a sign that the quench crosses from the CP. Further, as shown, the amount of the steady state for the quench of large size and crossed from the CP is lower than all which indicates the decrease of entanglement of initial entangled pairs (Fig. 5(b)). In contrast, QD first decreases as time increase for all quenches performed near to, into, and far away from the CP. For quenches crossed from the CP and into a region $0.5 \leqslant h_f \leqslant 1.0$, the QD after dropping to its minimum, increases rapidly and starts fluctuating around its saturated value. However, for large size quenches far away from the CP, the system gets more stable with lower fluctuations (Fig. 5(d)). Moreover, one can also observe the amount of the steady state for quench to $h_f < h_c$ is lower than all with almost tiny oscillations.

In order to quantify the change of the many-body wave-function when the system crosses the CP, let us focus on the density-plots. Figs. 5(b & d) clearly display the behavior of concurrence for a quench around the CP is different from that of the QD. For quench to $h_f < h_c$ concurrence with the enhance of h_f enhances, near to CP ($h_f \approx h_c - \delta$ with $\delta \ll 1$) gets its maximum value, then for $h_f > h_c - \delta$ reduces. It means, the maximum of the concurrence does not occur exactly at the CP which demonstrates the out-of-equilibrium dynamics of concurrence is in a good agreement with zero-temperature phase transition [51]. On the other hand, the QD has a stable value for $h_f < h_c$ and starts to boost exactly at $h_f = h_c$.

More interesting is when the initial state of the system is in the PM phase, $h_i = 2.0$ (Figs. 5(e-h)). For all QCs around the CP as h_f: $0.7 \rightarrow 0.3$, first, from a nonzero value start to decrease with passing time, achieve thier minimum values, and finally by an increment commence to fluctuations and at enough large times tend to the given values. The survival of QCs happens when quenches cross from the CP. In a similar behavior for both concurrence and QD, as obviously is seen from Figs. 5(f & h), values of steady states of these two QCs for h_f: $1.9 \rightarrow 0.0$ at very long times reduce and put in their steady states.

As a consequence, these results for out-of-equilibrium dynamics imply while the indications of quantum phase transition for concurrence do not occur at the CP, still one can detect the quantum phase transitions via QD. Recently, an imprint of our results was done for the dynamical behaviors of QCs and their connections to quantum criticality for the 1D spin-1/2 XZZ model in the presence of transverse magnetic field [57].

Now, we are prepared to discuss about the effect of the frustration in the dynamics of QCs in ANNNI model. In Fig. 6 it is depicted concurrence and the QD for values of weak frustrations $\Delta = 0.1, 0.2, 0.3, 0.4$ (from red to black) for quench from $h_i = 0.1$ ((a) (b)) and $h_i = 2.0$ ((c) (d)). As is seen in Figs. 6(a & c), the concurrence shows the oscillatory decay with respect to the time for all values of the frustration, Δ. Although, no cusps are seen in the time behavior of the concurrence, the QD between nearest pair spins, Figs. 6(b & d) show

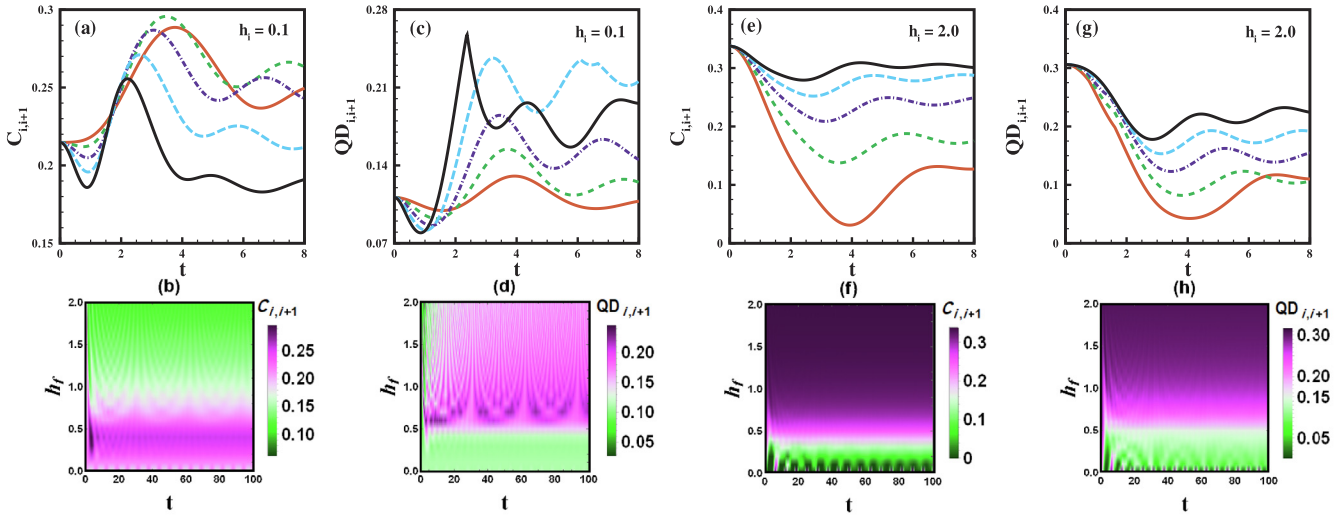

Fig. 5. The time evolution of concurrence and quantum discord, and also their density-plots as a function of time and final magnetic field h_f for the first neighbor spin pairs for quench (a-d) from $h_i = 0.1$, and (e-h) from $h_i = 2.0$ to $h_f = [0.3, 0.7]$ (from red to black) and desired h_f respectively. (For interpretation of the references to colour in this figure legend, the reader is referred to the web version of this article.)

explicit cusps by passing time, which can be considered as the capability of the QD for studying the DQPT with respect to the concurrence. Notely, our results indicate that the time to occur cusps differ from t^*. For example for quench from $h_i = 2.0$ to $h_f = 0.1$ at $\Delta = 0.4$ where the quenched point is close to the CP, only one cusp appears (Fig. 6(d)). Similar to this situation to the emerge of cusps can also be seen in Ref.[57] where for the 1D spin-1/2 XZZ model quenches are crossed from the critical anisotropy parameter. However, Figs. 6(a & b) exhibit for quench from FM to PM, enhancing values of the frustration enhances values of QCs. An interesting event happens for concurrence when quench is done from $h_i = 2.0$. In this case, increasing the amount of the frustration decreases the time of the sudden death for a given interval time evolution of the system so that for $\Delta = 0.4$, as shown in Fig. 6(c), it prevents occurring of sudden death in the system.

5. Conclusion

The examination of the dynamics of non-integrable systems is appealing, in spite of its complication. One way to consider these systems is the use of the mean-field approach. It helps us with a fermionic picture together with Wick's theorem to diagonalize the Hamiltonian 1D spin-1/2 transverse axial next-nearest-neighbor Ising model where the next-nearest neighbor interaction breaks the integrability. This leads to the five self-consistent equations which will be solved numerically. It is known when signs of coupling interactions of NN and NNN differ, in the system the frustration emerges. On the other note, it was shown for this model the mean-field Jordan-Wigner approach works very well when the value of the frustration is low [28]. Therefore, here, we restrict ourself to the value of the weak frustration ($\Delta < 0.5$).

In this work, we have implemented the idea of dynamical quantum phase transition to study out-of-equilibrium dynamics of ANNNI model. The DQPTs arise at non-analyticity of the rate function in the critical times where the wave number has the special value k^*. We have shown the boost of the frustration enhances the k^* such a way that k^* has approximate a linear relation with Δ. Moreover, we have presented the impact of the frustration at the passing time of rate function so that while it leads to the greater fluctuations for quench from FM to PM, in a contrary way, it leads to the smaller fluctuations for quench from PM to FM. For all quenches crossed from critical points, the non-analyticities are indicated. An important result in this part was affirming the existence of PC and PI phases in the system.

We have also studied dynamics of spin–spin correlation function $S^{xx}_{n,n+1}(t) = < S^x_n(t) S^x_{n+1}(t) >$ as an order parameter of the system and the magnetization $M_z(t)$. Our results demonstrate these two parameters for quench from PM to FM behave initially different in such a way that with passing time the absolute value of $M_z(t)$ increases but $S^{xx}_{n,n+1}(t)$ decreases. For this case, the influence of the frustration demolishes the fluctuations and causes reaching a stable state sooner. On the other side, for a quench from FM to PM the frustration precludes to achieve the stable state even at $t \to \infty$.

As we know, the dynamics of quantum correlations in closed many-body systems show several interesting features to detect distinctive phases especially when we deal with non-integrable systems or systems

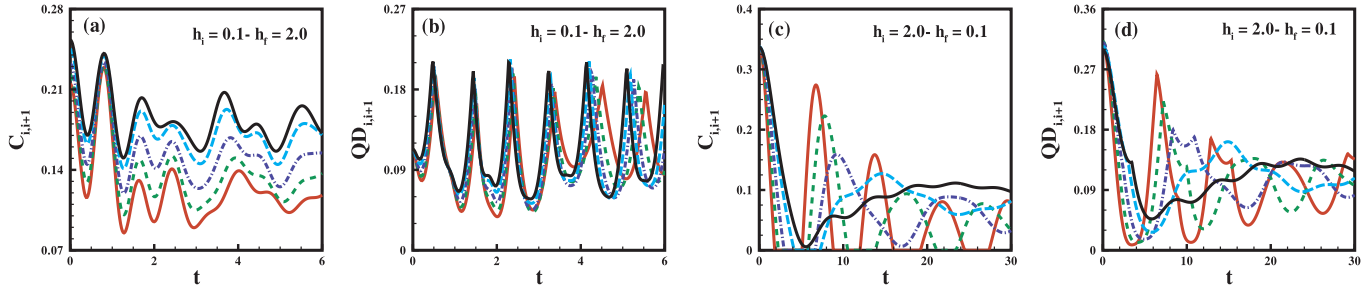

Fig. 6. The time evolution of the concurrence and the quantum discord between nearest neighbor spins in a quench from (a & b) FM phase into the PM phase and (c & d) PM phase into the FM phase. Different values of the frustration are considered as Δ: 0.0 → 0.4 (from red to black). (For interpretation of the references to colour in this figure legend, the reader is referred to the web version of this article.)

with complicated phase-diagram. Here we have employed the bipartite quantum discord and concurrence as two powerful measurement tools. To get a clear notion of behaviors of these two QCs, first of all, we have approved our study for the ITF model. The results are in a good agreement with zero-temperature phase transition and imply while the concurrence does not reveal the exact critical points, still QD does. In addition, the initial behavior of QD for all quenches is as descending. Further, the concurrence has the same initial behavior for quench from PM or FM to PM. One more, for both the absence and the presence of the frustration, our outcomes show for quenches crossed from the critical point the cusps arise from QD. This manifests that dynamics of QD could be as the fingerprint of DQPTs. The influence of the frustration is exciting where for dynamics of concurrence at $\Delta = 0.4$ for quench from $h_i = 2.0$ to $h_f = 0.1$ this leads to eliminate the sudden death. It concludes that the present technique ables us to study the silent features of the dynamics of non-integrable quantum systems.

Finally, we have to mention that the J-W mean-field approximation is only the first attempt to describe the dynamical quantum phase transition in the mentioned model in the view of the frustration. For getting an imprint of this technique we suggest that it would be better our results are also checked with other powerful methods such as DMRG.

Acknowledgments

H. Cheraghi's acknowledges Iran Science Elites Federation for partial financial support. Also, H. Cheraghi is very grateful to Prof. Christoph Karrasch for sending the DMRG data in Fig. 1.

Appendix A

The elements of the reduced matrix are

$$\begin{aligned}
X^{+}_{i,i+m}&=\langle n_i n_{i+m}\rangle,\\
X^{-}_{i,i+m}&=\langle 1-n_i-n_{i+m}+n_i n_{i+m}\rangle,\\
Y^{+}_{i,i+m}&=\langle n_i(1-n_{i+m})\rangle,\\
Y^{-}_{i,i+m}&=\langle n_{i+m}(1-n_i)\rangle,\\
Z_{i,i+m}&=\left\langle a_i^{\dagger}\left(\prod_{l=i}^{i+m-1}\left(1-2a_l^{\dagger}a_l\right)\right)a_{i+m}\right\rangle,\\
f_{i,i+m}&=\left\langle a_i^{\dagger}\left(\prod_{l=i}^{i+m-1}\left(1-2a_l^{\dagger}a_l\right)\right)a_{i+m}^{\dagger}\right\rangle.
\end{aligned} \tag{27}$$

Therefore, the concurrence of the density matrix is given by

$$C(\rho_{i,i+m}) = Max[0, \Lambda_1, \Lambda_2], \tag{28}$$

where

$$\begin{aligned}
\Lambda_1&=2(|Z_{i,i+m}| - (X^{+}_{i,i+m}X^{-}_{i,i+m})^{1/2}),\\
\Lambda_2&=2(|f_{i,i+m}| - (Y^{+}_{i,i+m}Y^{-}_{i,i+m})^{1/2}).
\end{aligned} \tag{29}$$

In addition, QD is defined by difference of total correlation, $\mathscr{I}(\rho_{i,i+m})$, and classical correlation, $\mathscr{C}(\rho_{i,i+m})$. The total correlation can be calculated by

$$\mathscr{I}(\rho_{i,i+m}) = S(\rho_i) + S(\rho_{i,i+m}) + \sum_{\alpha=0}^{3}\lambda_\alpha \log_2\lambda_\alpha, \tag{30}$$

where λ_α is the eigenvalue of the density matrix $\rho_{i,i+m}$, and

$$S(\rho_i) = -\sum_{\xi=\pm1}\left[\frac{1+\xi c_4}{2}\log_2\left(\frac{1+\xi c_4}{2}\right)\right]. \tag{31}$$

Here, $c_{i=1,\ldots,4}$, are expressed as

$$\begin{aligned}
c_{1/2}&=2(Z_{i,i+j} \pm f_{i,i+m}),\\
c_{3/4}&=X^{+}_{i,i+m} \pm X^{-}_{i,i+m} - Y^{+}_{i,i+m} \mp Y^{-}_{i,i+m}.
\end{aligned} \tag{32}$$

Since the translation invariance of the original Hamiltonian, the single-site density matrices ρ_i and $\rho_{i,i+m}$ are equal, therefore, we have $S(\rho_i) = S(\rho_{i,i+m})$.

The calculation of the classical correlation $\mathscr{C}(\rho_{i,i+m})$ requires an optimization over rank-1 local measurements on part B of $\rho_{i,i+m}$ (here we have taken site j of $\rho_{i,j}$ as part B). A general set of local rank-1 measurement operators, B_0, B_1, can be defined as $B_{k'=0/1} = V\prod_{k'}V^{\dagger}$, where $V \in U(2)$ and the projectors $\prod_{k'}$ are given in the computational basis $|0\rangle \equiv |\uparrow\rangle$ and $|1\rangle \equiv |\downarrow\rangle$. The post measurement outcomes get updated to one of the following states

$$\rho_{k'} = \left(\frac{1}{2} + \sum_{j=1}^{3}\chi_{k'}S_j\right)\otimes\left(V\prod_{k'}V^{\dagger}\right), \tag{33}$$

where the elements of the density matrices are given by

$$\chi_{k'i=1,2}=\frac{(-1)^{k'}c_i\sin\theta\cos\phi}{1+(-1)^{k'}c_4\cos\theta},$$
$$\chi_{k'3}=\frac{(-1)^{k'}c_3\cos\theta+c_4}{1+(-1)^{k'}c_4\cos\theta}. \quad (34)$$

Here the azimuthal angle $\theta=[0,\pi]$ and the polar angle $\phi=[0,2\pi]$ represent a qubit over the Bloch sphere. By considering the normalization of the density matrices, $\theta_{k'}=\left(\sum_{j=1}^{3}\chi_{k'j}^2\right)^{1/2}$, we finally arrive to the classical correlation between the spin pairs

$$\mathscr{C}(\rho_{i,i+m})=Max_{\{B_{k'}\}}\left[S(\rho_i)-\frac{S(\rho_0)+S(\rho_1)}{2}c_4\cos\theta\frac{S(\rho_0)-S(\rho_1)}{2}\right], \quad (35)$$

where the von Neumann entropies are identified as

$$S(\rho_{k'})=-\sum_{\xi=\pm1}\left[\frac{1+\xi\theta_{k'}}{2}\log_2\left(\frac{1+\xi\theta_{k'}}{2}\right)\right]. \quad (36)$$

Note that the von Neumann entropy of $V\prod_{k'}V^{\dagger}$ is zero. All needed parameters to calculate of two sites reduced density matrix will be obtained from (25) and (26).

Appendix B. Supplementary data

Supplementary data associated with this article can be found, in the online version, athttps://doi.org/10.1016/j.jmmm.2019.166078.

References

[1] A. Peres, Phys. Rev. A 30 (1984) 1610.
[2] M. Heyl, A. Polkovnikov, S. Kehrein, Phys. Rev. Lett. 110 (13) (2013) 135704 .
[3] M. Heyl, Rep. Prog. Phys. 81 (2018) 054001 .
[4] M. Heyl. arXiv:1811.02575.
[5] M. Heyl, M. Vojta, Phys. Rev. B 92 (2015) 104401 .
[6] J.S. Caux, F.H. Essler, Phys. Rev. Lett. 110 (2013) 257203 .
[7] S. Sharma, U. Divakaran, A. Polkovnikov, A. Dutta, Phys. Rev. B. 93 (2016) 144306 .
[8] N.O. Abeling, S. Kehrein, Phys. Rev. B. 93 (2016) 104302 .
[9] M. Heyl, Phys. Rev. B. 95 (2017) 060504(R).
[10] D. Trapin, M. Heyl, Phys. Rev. B. 97 (2018) 174303 .
[11] M. Heyl, Phys. Rev. Lett. 113 (2014) 205701 .
[12] F. Andraschko, J. Sirker. Phys. Rev. B. 89 (2014) 125120 .
[13] B. Wouters, J. De Nardis, M. Brockmann, D. Fioretto, M. Rigol, J.S. Caux, Phys. Rev. Lett. 113 (2014) 117202 .
[14] M. Brockmann, B. Wouters, D. Fioretto, J. De Nardis, R. Vlijm, J.S. Caux, J. Stat. Mech.: Theory Exp. 2014 (12) (2014) P12009.
[15] P.P. Mazza, J.M. Stephan, E. Canovi, V. Alba, M. Brockmann, M. Haque, J. Stat. Mech.: Theory Exp. 2016 (1) (2016) 013104 .
[16] L. Piroli, B. Pozsgay, E. Vernier, Nucl. Phys. B 933 (2018) 454–481.
[17] S. Vajna, B. Dóra, Phys. Rev. B. 89 (2014) 161105(R).
[18] J.L. Lancaster, Phys. Rev. E. 93 (2016) 052136 .
[19] M. Lacki, M. Heyl. arXiv:1812.02209.
[20] P. Jurcevic, H. Shen, P. Hauke, C. Maier, T. Brydges, C. Hempel, B.P. Lanyon, M. Heyl, R. Blatt, C.F. Roos, Phys. Rev. Lett. 119 (2017) 080501 .
[21] J. Zhang, G. Pagano, P.W. Hess, A. Kyprianidis, P. Becker, H. Kaplan, A.V. Gorshkov, Z.X. Gong, C. Monroe, Nature 551 (2017) 601.
[22] N. Fläschner, D. Vogel, M. Tarnowski, B.S. Rem, D.S. Lühmann, M. Heyl, J.C. Budich, L. Mathey, K. Sengstock, C. Weitenberg, Nature Physics 14 (2018) 265.
[23] M.E. Fisher, W. Selke, Phys. Rev. Lett. 44 (1980) 1502.
[24] I. Peschel, V.J. Emery, Zeitschrift für Physik B Condensed Matter 43 (3) (1981) 241–249.
[25] W. Selke, Phys. Rep. 170 (4) (1988) 213–264.
[26] P. Sen, B.K. Chakrabarti, Phys. Rev. B 40 (1989) 760.
[27] C.M. Arizmendi, A.H. Rizzo, L.N. Epele, C.G. Canal, Z. Phys. B: Condens. Matter 83 (2) (1991) 273–276.
[28] P. Sen, S. Chakraborty, S. Dasgupta, B.K. Chakrabarti, Z. Phys. B: Condens. Matter 88 (1992) 333.
[29] H. Rieger, G. Uimin, Z. Phys. B: Condens. Matter 101 (4) (1996) 597–611.
[30] M. Beccaria, M. Campostrini, A. Feo, Phys. Rev. B 73 (5) (2006) 052402 .
[31] M. Beccaria, M. Campostrini, A. Feo, Phys. Rev. B 76 (9) (2007) 094410 .
[32] A.K. Chandra, S. Dasgupta, Phys. Rev. E 75 (2) (2007) 021105 .
[33] A. Nagy, New J. Phys. 13 (2) (2011) 023015 .
[34] S. Suzuki, J.I. Inoue, B.K. Chakrabarti, Quantum Ising phases and transitions in transverse Ising models vol. 862, Springer, 2012.
[35] O.F. de Alcantara Bonfim, B. Boechat, J. Florencio. Phys. Rev. E 96 (4) (2017) 042140 .
[36] C. Karrasch, D. Schuricht, Phys. Rev. B 87 (19) (2013) 195104 .
[37] J.N. Kriel, C. Karrasch, S. Kehrein, Phys. Rev. B 90 (12) (2014) 125106 .
[38] D.M. Kennes, D. Schuricht, C. Karrasch, Phys. Rev. B 97 (18) (2018) 184302 .
[39] M. Heyl, F. Pollmann, B. Dóra, Phys. Rev. Lett. 121 (1) (2018) 016801 .
[40] S. Sachdev, Quantum Phase Transitions, Cambridge University Press, 9780521514682, 2001.
[41] E. Lieb, T. Schultz, D. Mattis, Ann. Phys. 16 (3) (1961) 407–466.
[42] M.E. Fisher, Boulder Lectures in Theoretical Physics vol. 7, University of Colorado, Boulder, 1965.
[43] C.N. Yang, T.D. Lee, Phys. Rev. 87 (3) (1952) 404.
[44] F. Andraschko, J. Sirker. Phys. Rev. B. 89 (2014) 125120 .
[45] H. Cheraghi, S. Mahdavifar, J. Phys.: Condensed Matter 30 (42) (2018) p. 42LT01.
[46] B. Zunkovic, M. Heyl, M. Knap, A. Silva, Phys. Rev. Lett 120 (13) (2018) 130601 .
[47] A. Silva, Phys. Rev. Lett. 101 (12) (2008) 120603 .
[48] P. Calabrese, F.H. Essler, M. Fagotti, Phys. Rev. Lett. 106 (22) (2011) 227203 .
[49] D.A. Wisniacki, Phys. Rev. E 67 (1) (2003) 016205 .
[50] A. Goussev, R.A. Jalabert, H.M. Pastawski, D. Wisniacki. arXiv preprint arXiv:1206.6348 (2012).
[51] A. Osterloh, L. Amico, G. Falci, R. Fazio, Nature 416 (6881) (2002) 608.
[52] T.J. Osborne, M.A. Nielsen, Phys. Rev. A 66 (3) (2002) 032110 .
[53] S.J. Gu, S.S. Deng, Y.Q. Li, H.Q. Lin, Phys. Rev. Lett. 93 (8) (2004) 086402 .
[54] R. Dillenschneider, Phys. Rev. B. 78 (22) (2008) 224413 .
[55] Z. Shadman, H. Cheraghi, S. Mahdavifar, Phys. A: Stat. Mech. Appl. 512 (2018) 1128–1139.
[56] T. Werlang, C. Trippe, G.A.P. Ribeiro, G. Rigolin, Phys. Rev. Lett. 105 (9) (2010) 095702 .
[57] U. Mishra, H. Cheraghi, S. Mahdavifar, R. Jafari, A. Akbari, Phys. Rev. A 98 (5) (2018) 052338 .
[58] P. Hauke, L. Tagliacozzo, Phys. Rev. Lett. 111 (20) (2013) 207202 .
[59] M. Fagotti, M. Collura. arXiv preprint arXiv:1507.02678 (2015).
[60] F.H. Essler, S. Evangelisti, M. Fagotti, Phys. Rev. Lett. 109 (24) (2012) 247206 .
[61] P. Calabrese, F.H. Essler, M. Fagotti, J. Stat. Mech.: Theory Exp. 2012 (07) (2012) P07016.
[62] G. Torlai, L. Tagliacozzo, G. De Chiara, J. Stat. Mech.: Theory Exp. 2014 (6) (2014) P06001.
[63] S. Hill, W.K. Wootters, Phys. Rev. Lett. 78 (26) (1997) 5022.
[64] W.K. Wootters, Phys. Rev. Lett. 80 (10) (1998) 2245.
[65] H. Ollivier, W.H. Zurek, Phys. Rev. Lett. 88 (1) (2001) 017901 .
[66] F.K. Fumani, S. Nemati, S. Mahdavifar, A.H. Darooneh. 445, pp. 256–263 (2016).
[67] M.S. Sarandy, Phys. Rev. A 80 (2) (2009) 022108 .